AJNR

Evaluation of intracranial lesions with inversion recovery half-Fourier single-shot turbo spin-echo MR: initial observations.

I Ikushima, Y Korogi, Y Yamashita, T Yi, S Hamatake, T Sugahara, Y Shigematsu and M Takahashi

AJNR Am J Neuroradiol 1997, 18 (3) 421-426
http://www.ajnr.org/content/18/3/421

Evaluation of Intracranial Lesions with Inversion Recovery Half-Fourier Single-Shot Turbo Spin-Echo MR: Initial Observations

Ichiro Ikushima, Yukunori Korogi, Yasuyuki Yamashita, Tang Yi, Satoshi Hamatake, Takeshi Sugahara, Yoshinori Shigematsu, and Mutsumasa Takahashi

PURPOSE: To determine the value of inversion recovery half-Fourier single-shot turbo spin-echo (IR-HASTE) MR sequences in the characterization of a variety of intracranial lesions, with the focus on differentiating between epidermoids and nonneoplastic cystic lesions. **METHODS:** We used a 1.5-T MR unit to study five epidermoids, seven arachnoid cysts, seven other nonneoplastic cysts (three neuroepithelial cysts, two interhemispheric cysts, and two Rathke's cleft cysts), and eight solid neoplasms (three meningiomas, two astrocytomas, one subependymoma, one cavernoma, and one metastatic tumor) using IR-HASTE sequences with variable inversion times (TI). Imaging time for each section was 2 seconds for the sequence. The TI nulling values were analyzed statistically. **RESULTS:** The TI nulling values were 1200 to 2300 for the epidermoids, 2800 to 3000 for the arachnoid cysts, 300 and 800, respectively, for the Rathke's cleft cysts, 2500 to 3000 for the other nonneoplastic cysts, and 300 to 1500 for the solid neoplasms. There was no overlap of TI nulling values between the arachnoid cysts and the epidermoids; the difference was statistically significant. Both patients with interhemispheric cysts had two lesions in which the TI nulling values were different. **CONCLUSION:** IR-HASTE sequences provide a rapid and reliable imaging method for differentiating among epidermoids, arachnoid cysts, and solid neoplasms. This technique also provides information about the continuity of the multicystic lesions in terms of the differences in their TI nulling values. For solid intraaxial masses, the use of IR-HASTE helps to differentiate intratumoral cysts and necrosis from solid components.

Index terms: Brain neoplasms, magnetic resonance; Magnetic resonance, technique

AJNR Am J Neuroradiol 18:421–426, March 1997

The inversion recovery (IR) sequence of magnetic resonance (MR) imaging can be used to detect disease in the central nervous system. A short inversion time (TI) IR sequence can be used to suppress the signal from orbital fat with little residual signal and to detect the lesions in the optic nerve with good contrast (1). Medium-TI IR sequences provide information about the location of the disease, enable an assessment of the mass effect, and supply developmental information in older infants. The medium-TI IR sequence is also a good technique for computing T1 maps (2, 3). Long-TI IR sequences help to distinguish tumor from edema. In particular, the fluid-attenuated inversion-recovery sequence, which nulls the signal from cerebrospinal fluid (CSF) and produces very heavy T2-weighted images as a consequence of the very long echo time, has recently been reported to be more sensitive for the detection of abnormal lesions in several neurologic disorders than are conventional T1- and T2-weighted images (4–8).

The half-Fourier single-shot turbo spin-echo (HASTE) sequence is a high-speed heavily T2-weighted acquisition with an echo train length (ETL) of 128 obtained in an imaging time of approximately 2 seconds (single shot) (9). HASTE sequences have been used successfully for MR cholangiopancreatography (10) (J. C. Sananes, M. Bonne, R. Lecesn, et al, "Magnetic Resonance Cholangiography using HASTE Sequence: Optimization and Clinical Evaluation in Extrahepatic Cholestasis," In: *Pro-*

Received May 29, 1996; accepted after revision September 23.

From the Department of Radiology, Kumamoto University School of Medicine, 1–1–1 Honjo, Kumamoto 860, Japan. Address reprint requests to Ichiro Ikushima MD.

AJNR 18:421–426, Mar 1997 0195-6108/97/1803–0421

ceedings of the Society of Magnetic Resonance, Volume 3: Third Scientific Meeting and Exhibition, Nice, France, August 1995) or MR cisternography. By combining the IR sequence with the HASTE sequence (IR-HASTE), the lesions can be selectively suppressed according to the tissue-specific TI in a short imaging time (approximately 2 seconds).

The purpose of this study was to determine the value of IR-HASTE sequences in the diagnosis of various intracranial lesions, focusing on the differentiation of epidermoids from nonneoplastic cystic lesions by means of the tissue-specific nulling TI obtained with this sequence.

Materials and Methods

The study population consisted of 27 patients in whom the following were found: five epidermoids, seven arachnoid cysts, seven other nonneoplastic cysts (three neuroepithelial cysts, two interhemispheric cysts, two Rathke's cleft cysts), and eight intracranial solid neoplasms (three meningiomas, two astrocytomas, one subependymoma, one cavernoma, and one metastatic brain tumor). Sixteen patients were male and 11 were female; ages ranged from 4 to 71 years (mean, 46 years). The epidermoids ranged from 1.5 to 6.5 cm in diameter; two were located in the cerebellopontine angle cistern, two in the prepontine cistern, and one in the left middle cranial fossa. The arachnoid cysts varied from 1.5 to 4.7 cm in diameter. Five were located in the middle cranial fossa, one in the posterior fossa, and one in the cerebellopontine angle cistern. The three neuroepithelial cysts varied from 0.5 to 3.5 cm in diameter; two were located in lateral ventricles and one in a choroidal fissure. The two Rathke's cleft cysts were 2.2 and 2.5 cm in diameter, respectively, and the two interhemispheric cysts were 2.0 and 4.2 cm in diameter, respectively. The solid neoplasms ranged from 2.0 to 5.5 cm in diameter: two were located in the frontal lobe, two in the temporal lobe, two in the cerebellum, one in a cavernous sinus, and one in a lateral ventricle. The diagnoses of epidermoid and intracranial solid neoplasm were proved surgically and that of nonneoplastic cysts was established by the location of the lesion, the MR signal intensity, and the absence of enhancement after administration of contrast medium on T1-weighted images.

All studies were obtained on a 1.5-T superconductive unit equipped with a standard transmit-receive head coil. IR-HASTE sequences were obtained with one excitation and an ETL of 128 (Fig 1). Single-section images were obtained in the transverse plane with a 5-mm section thickness and a matrix of 128 × 256 and reconstructed by use of the half-Fourier transform technique. A series of TI values was employed to find the specific value that would null or decrease the signal intensity of each lesion. In all cases, images were obtained with variable TI values, ranging from 200 to 3000. To start, a TI value of 3000 was applied, which is the null point of CSF; then the TI was decreased in increments of 100 milliseconds. When the signal intensity of the lesion at a given TI value became greater than that at the previous value, the previous value was adopted as the TI nulling value. For each imaging study, the data acquisition time was 2 seconds.

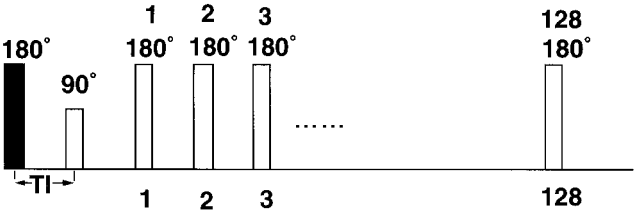

Fig 1. In the HASTE sequence, a single excitation pulse is used to obtain all image information. After the sections are excited, up to 128 echoes are generated using multiple 180° pulses. The first echo of the multiecho pulse train is encoded using a small phase-encoding gradient. The gradient strength is then sequentially lowered from echo to echo to the highest negative amplitude; consequently, only slightly more than half the raw data are acquired. The image was obtained using a half-Fourier reconstruction, the TE was 87, TIs of 200 to 3000 were tested to find tissue-specific nulling value, section thickness was 5 mm, and acquisition time was 2 seconds. In this type of acquisition, an inversion pulse is used before the HASTE sequence. TI is designated as the interval between the 180° pulse and the 90° pulse.

Before applying the IR-HASTE sequence, we examined the entire brain with a T1-weighted (670/14 [repetition time/echo time]) spin-echo (SE) sequence and a T2-weighted turbo SE sequence (4500/96, ETL = 7). The anatomic level at which the lesion was of maximum diameter was identified. After applying the IR-HASTE sequence, we performed T1-weighted SE MR imaging with contrast enhancement (0.1 mmol/kg of body weight). The phase-encoding direction was right to left for all sequences.

To determine the null point of CSF, we conducted a preliminary phase study in three healthy volunteers. In each case, images were obtained with the use of the variable TI values: 2800, 2900, 3000, 3100, and 3200. For the IR-HASTE sequence, we estimated the difference in TI nulling values among epidermoids, arachnoid cysts, neuroepithelial cysts, interhemispheric cysts, Rathke's cleft cysts, and solid neoplasms. The continuity of multiple cysts was estimated by the difference in their TI nulling values.

For the quantitative analysis of epidermoids and arachnoid cysts, we obtained an IR-HASTE sequence at the null point of CSF, where the signal-to-noise (S/N) ratios of the lesions were calculated as follows: S/N = signal intensity of lesion/standard deviation of noise. To minimize partial volume effects, we selected the image that showed the maximum area of the lesion and used a circular region of interest (ROI) that approached but did not exceed the lesion's margin. The signal intensity in the ROI was measured in all lesions by the same investigator. CSF signal intensities were measured with the same size ROI as that selected in the lesions. Background noise was measured

with a large ROI cephalad to the head. For hypothesis testing, the data were analyzed statistically using an unpaired *t* test.

Results

For the three volunteers, mean S/N ratios of CSF at TI values of 2800, 2900, 3000, 3100, and 3200 were 2.99 ± 0.12, 2.27 ± 0.42, 1.80 ± 0.34, 2.02 ± 0.18 and 3.47 ± 0.71, respectively. A TI value of 3000 was chosen as the null point of CSF. At this value, the mean S/N ratio of epidermoids was 21.1 ± 8.5 and that of arachnoid cysts was 0.4 ± 1.5; this difference was statistically significant ($P < .01$).

TI nulling values of intracranial lesions with an IR-HASTE sequence

Type of Lesion	n	TI Nulling Value	
Epidermoids	5	1800 ± 320 (1200–2300)	$P < .01$
Arachnoid cysts	7	2957 ± 61 (2800–3000)	
Interhemispheric cysts	4	2750 ± 250 (2500–3000)	
Neuroepitherial cysts	3	2833 ± 222 (2500–3000)	
Rathke cleft cysts	2	800, 300	$P < .01$
Solid neoplasms	8	957 ± 265 (300–1500)	

The TI nulling values of various intracranial lesions are summarized in the Table and illustrated in Figures 2 through 5. There was no overlap of the TI nulling values between epidermoids and arachnoid cysts, and the difference was statistically significant ($P < .01$). A statistically significant difference in TI nulling values also was found between epidermoids and interhemispheric cysts ($P < .01$), between epidermoids and neuroepithelial cysts ($P < .01$), between epidermoids and Rathke's cleft cysts ($P < .03$), and between epidermoids and solid neoplasms ($P < .01$). There were no significant differences in T1 nulling values between arachnoid cysts, interhemispheric cysts, and neuroepithelial cysts. Although the TI nulling value of epidermoids was significantly higher than that of solid neoplasms, there was some overlap between them.

The two interhemispheric cysts had TI nulling values of 2500 and 3000, respectively (Fig 4). Among the eight patients with solid intraaxial masses, three had intratumoral cysts or necrosis on MR images. Two of these cysts had a TI

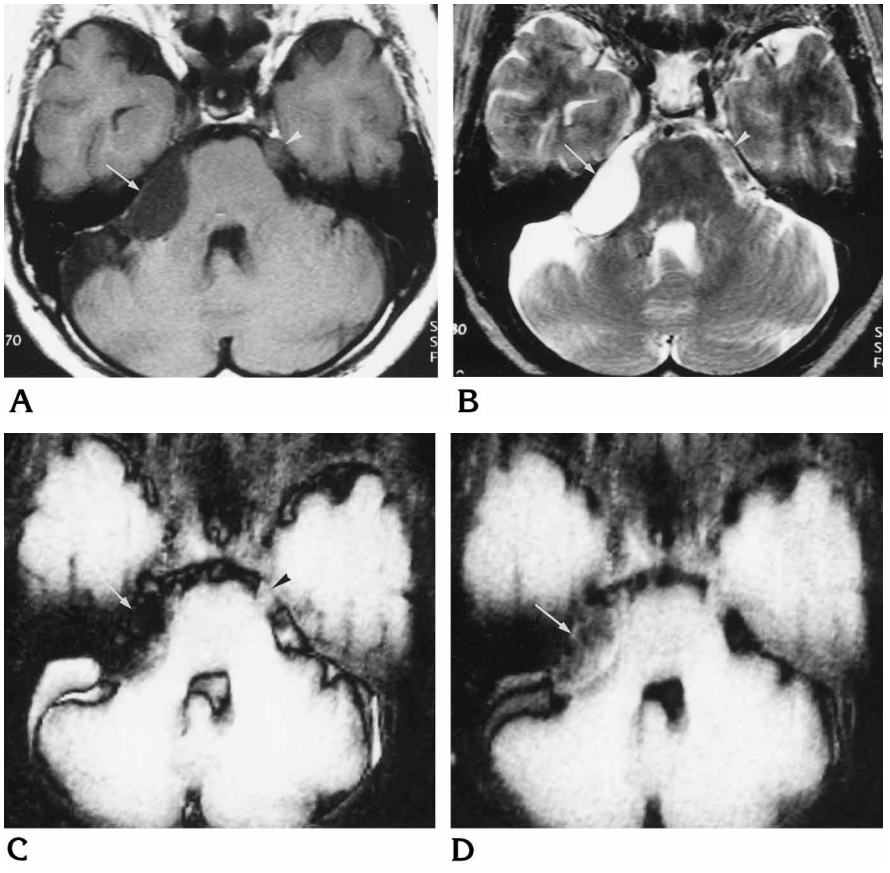

Fig 2. A 71-year-old woman with bilateral epidermoids in the cerebellopontine angles.

A, On T1-weighted SE image (670/14/1) the tumor in the right cerebellopontine angle cistern is nearly isointense with CSF (*arrow*). The small tumor in the left cerebellopontine angle cistern is hyperintense relative to CSF (*arrowhead*).

B, On T2-weighted turbo SE image (4500/96/2, ETL = 7) the tumor in the right cerebellopontine angle cistern is isointense with CSF (*arrow*). The tumor in the left cerebellopontine angle cistern is hypointense relative to CSF (*arrowhead*).

C, IR-HASTE image at a TI of 2000 depicts the nulling effect on the signal intensity of the tumor (*arrow*) in the right cerebellopontine angle cistern. The tumor on the left is hyperintense relative to CSF (*arrowhead*).

D, IR-HASTE image at a TI of 3000 depicts the nulling effect on the signal intensity of the CSF; the tumor on the right is hyperintense relative to CSF (*arrow*).

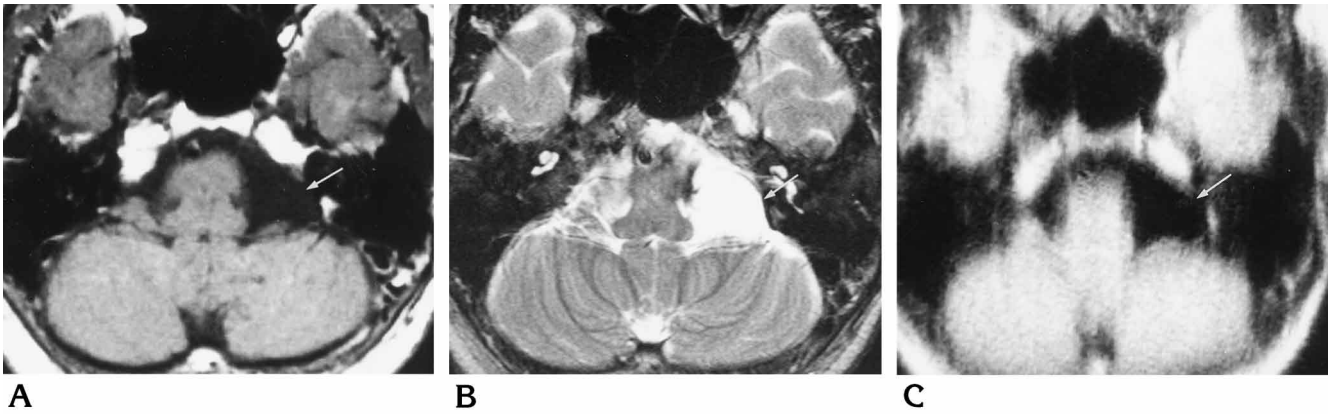

Fig 3. A 57-year-old woman with arachnoid cyst in the left pontomedullary region.
A, On T1-weighted SE image (670/14/1) the lesion is isointense with CSF (*arrow*).
B, On T2-weighted turbo SE image (4500/96/2, ETL = 7) the lesion is isointense with CSF (*arrow*).
C, IR-HASTE image at a TI of 3000 depicts the nulling effect on the signal intensity of the lesion (*arrow*) and CSF.

Fig 4. A 6-year-old boy with agenesis of the corpus callosum and two interhemispheric cysts.
A, On T1-weighted SE image (670/14/1) the medial cystic lesion is slightly hyperintense relative to CSF (*arrow*) and the lateral lesion is isointense with CSF (*arrowheads*).
B, On HASTE image, both lesions are isointense with CSF.
C, IR-HASTE image at a TI of 3000 depicts the nulling effect on the signal intensity of the lateral lesion (*arrowheads*) and CSF.
D, IR-HASTE image at a TI of 2500 depicts the nulling effect on the signal intensity of the medial lesion (*arrow*).

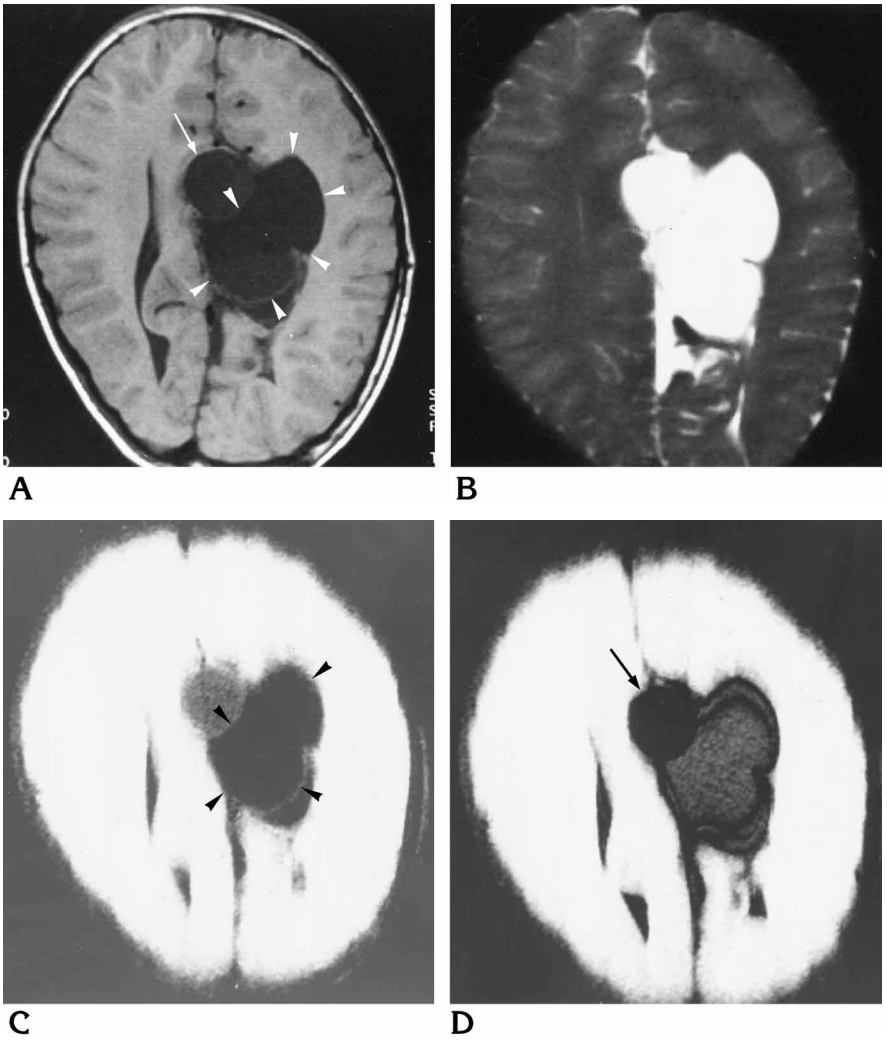

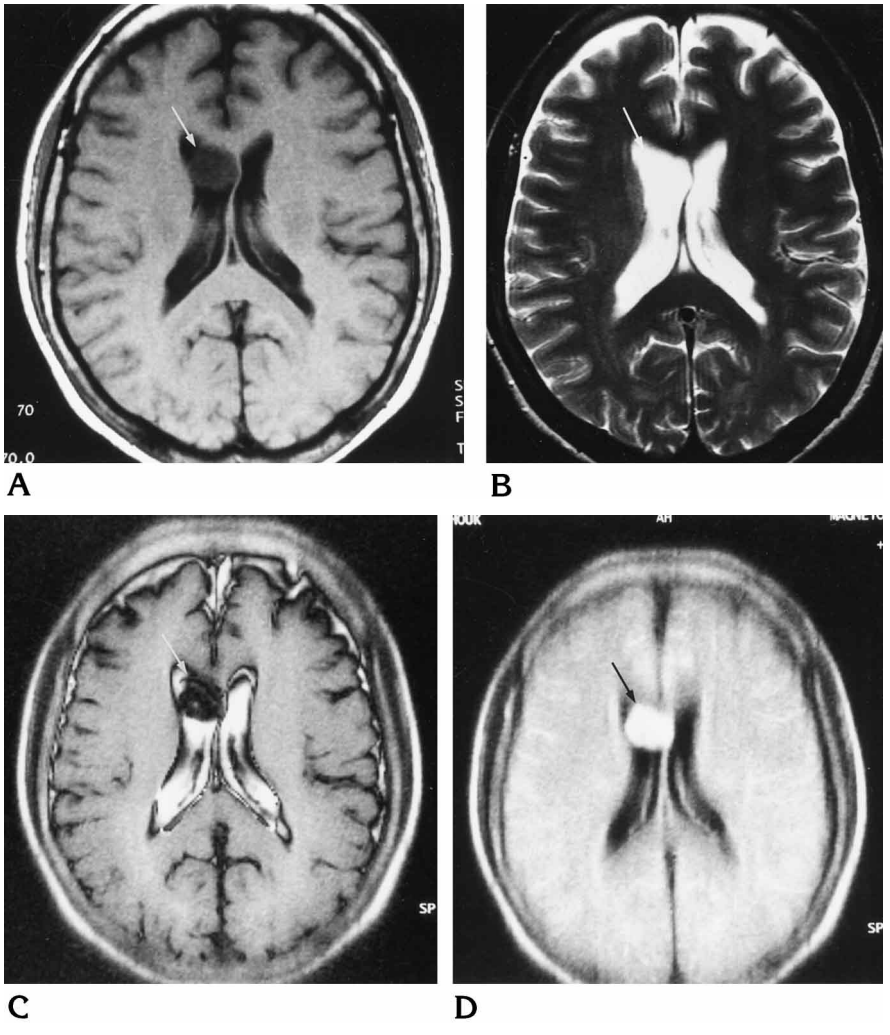

Fig 5. A 61-year-old woman with subependymoma in right lateral ventricle.

A, On T1-weighted SE image (670/14/1) the tumor in the right lateral ventricle is slightly hyperintense relative to CSF (*arrow*).

B, On T2-weighted turbo SE image (4500/96/2, ETL = 7) the tumor is isointense with CSF (*arrow*).

C, IR-HASTE image at a TI of 1500 depicts the nulling effect on the signal intensity of the tumor (*arrow*).

D, IR-HASTE image at a TI of 3000 depicts the nulling effect on the signal intensity of CSF. The tumor (*arrow*) is hyperintense relative to CSF.

nulling value of 3000; the other had a TI nulling value of 2400.

Discussion

At MR imaging, epidermoids typically appear slightly hyperintense relative to CSF on T1-, T2-, and proton density–weighted SE sequences (11–13). However, the difference in signal intensity between epidermoids and CSF is small, and differentiation between epidermoids and arachnoid cysts is frequently difficult on conventional SE sequences. Steady-state free-precession images have been reported to be useful for showing epidermoids in the subarachnoid space (14).

In this study, we used the IR-HASTE sequence to differentiate among epidermoids, nonneoplastic cysts, and solid neoplasms. The HASTE sequence uses a half-Fourier turbo SE technique with an ETL of 128 to obtain heavily T2-weighted images in a single shot. Because of the T2 decay during data acquisition, tissue with a short T2 produces practically no signal in the echoes at the end of the pulse train, thus making HASTE ideal for imaging fluid-containing structures. The IR sequence provides the ability to selectively suppress the signal intensity of epidermoids and nonneoplastic cysts with the use of tissue-specific TI nulling value. The TI nulling value for epidermoids was 1800 ± 320, whereas for arachnoid cysts it was 2957 ± 61. Because HASTE is a sequence with a single shot and an ETL of 128, in addition to the half-Fourier transformation technique, there is no repetition time. Therefore, T1 recovery does not affect imaging time, resulting in very rapid data acquisition (approximately 2 seconds). Several TI values can be tested within a short time.

As shown by Bydder and Young (3), if the repetition time of the pulse sequence is long relative to the T1 of tissue (ie, > 3 T1), then the TI nulling value is a simple multiple (between 0.59 and 0.69) of T1. With shorter repetition times, this simple rule does not hold. Theoretically, TI nulling value is equal to 69% of T1 relaxation time when repetition time is long enough (> 5 T1) (15). In IR-HASTE sequences, because only one excitation is used and one section is acquired, repetition time can be regarded as an extremely long and constant value (>>5 T1). Therefore, the TI nulling value obtained by IR-HASTE sequences should be closer to the true in vivo TI nulling value. T1 value of CSF measured in a selected section at 1.5 T is 2650. According to this value, the theoretical TI nulling value is 1829. In our MR unit, the true TI nulling value of CSF was approximately 3000. Factors determining the observed differences between them may be attributed to maladjustment of the frequency field inhomogeneity and to the arbitrary assumption regarding the signal exponential T1 decay of tissue.

On the basis of our findings, we believe that the IR-HASTE sequence has two major applications for intracranial lesions. First, at a TI of 3000 (nulling value of CSF), it is possible to differentiate epidermoids from arachnoid cysts in approximately 2 seconds. If a local dilatation of the subarachnoid space with mass effect is observed, the IR-HASTE sequence is helpful. However, to know the exact extension of epidermoids, a sequence with higher spatial resolution, such as steady-state free precession or fluid-attenuated inversion-recovery, is required. Second, IR-HASTE sequences make it easy to ascertain the difference between TI nulling values in cystic lesions of the subarachnoid space or ventricles and CSF. If the TI nulling value of a cystic lesion is different from that of CSF or an adjacent cystic lesion, there may be no continuity between them.

References

1. Johnson G, Miller DH, MacManus D, et al. STIR sequences in NMR imaging of the optic nerve. *Neuroradiology* 1987;29:238–245
2. Gadian DG, Payne JA, Bryant DJ, Young IR, Carr DH, Bydder GM. Gadolinium-DTPA as a contrast agent in NMR imaging-theoretical projections and practical observations. *J Comput Assist Tomogr* 1985;9:242–251
3. Bydder GM, Young IR. MR imaging: clinical use of inversion recovery sequence. *J Comput Assist Tomogr* 1985;9:659–75
4. John NR, Charlotte AH, Roger CG, et al. Initial clinical experience in MR Imaging of the brain with a fast fluid-attenuated inversion-recovery pulse sequence. *Radiology* 1994;193:173–180
5. Noguchi K, Ogawa T, Inugami A, et al. MR of acute subarachnoid hemorrhage: a preliminary report of fluid-attenuated inversion-recovery pulse sequences. *AJNR Am J Neuroradiol* 1994;15: 1940–1943
6. Takanashi J, Sugita K, Fujii K, Niimi H. MR evaluation of tuberous sclerosis: increased sensitivity with fluid-attenuated inversion recovery and relation to severity of seizures and mental retardation. *AJNR Am J Neuroradiol* 1995;16:1923–1928
7. Hajnal JV, Bryant DJ, Kasuboski L, et al. Use of fluid attenuated inversion recovery (FLAIR) pulse sequences in MRI of brain. *J Comput Assist Tomogr* 1992;16:841–844
8. De Coene B, Hajnal JV, Gatehouse P, et al. MR of the brain using FLAIR pulse sequences. *AJNR Am J Neuroradiol* 1992;13:1555–1564
9. Kiefer B, Grassner J, Hausmann R. Image acquisition in a second with half-Fourier acquisition single shot turbo spin echo. *J Magn Reson Imaging* 1994;4(P):86–87
10. Miyazaki T, Yamashita Y, Tsuchigame T, Yamamoto H, Urata J, Takahashi M. MR cholangiopancreatography using HASTE (half Fourier single shot turbo spin echo) sequence. *AJR Am J Roentgenol* 1996;166:1297–1303
11. Tampieri D, Melanson D, Ethier R. MR imaging of epidermoid cysts. *AJNR Am J Neuroradiol* 1989;10:351–356
12. Vion DJ, Vincentelli F, Jiddane M, et al. MR imaging of epidermoid cysts. *Neuroradiology* 1987;29:333–338
13. Gao P, Osborn AG, Smirniotopoulos JG, Harris CP. Radiologic-pathologic correlation epidermoid tumor of the cerebellopontine angle. *AJNR Am J Neuroradiol* 1992;13:863–872
14. Sakamoto Y, Takahashi M, Ushio Y, Korogi Y. Visibility of epidermoid tumors on steady-state free precession images. *AJNR Am J Neuroradiol* 1994;15:1737–1744
15. Majumdar S, Orphanoudakis SC, Gmitro A, O'Donnell M, Gore JC. Errors in the measurements of T2 using multiple-echo MRI techniques, II: effects of static field inhomogeneity. *Magn Reson Med* 1986;3:563–574